THE ASTROPHYSICAL JOURNAL, 224: L67–L71, 1978 September 1

EVIDENCE FOR THE ZEEMAN EFFECT IN THE OH MASER EMISSION FROM W3 (OH)

J. M. MORAN, M. J. REID, AND C. J. LADA
Harvard-Smithsonian Center for Astrophysics

J. L. YEN
University of Toronto

AND

K. J. JOHNSTON AND J. H. SPENCER
E. O. Hulburt Center for Space Research, Naval Research Laboratory
Received 1978 April 24; accepted 1978 June 9

ABSTRACT

We mapped the maser emission toward W3 (OH) in the $^2\Pi_{3/2}$, $J = 5/2$, $F = 3 \rightarrow 3$ transition of OH at 5 cm wavelength with a three-element VLB interferometer having 0".01 resolution. Our map of the source shows the positions of 12 spectral features that are predominantly right-circularly polarized and 10 features that are predominantly left-circularly polarized. Each of the left-circularly polarized features can be spatially paired with a nearby right-circularly polarized feature. These results provide strong evidence for Zeeman splitting in the OH emission with inferred magnetic field strengths ranging from 2 to 9 milligauss. The condensations responsible for the maser features have masses of about 10^{-5} $M_\odot$, are probably fragments in a single large cloud, and are not associated with individual protostars. The cluster of features is aligned with the compact H II region and may be located either in an accretion shell around it or in the molecular cloud ahead of an extended shock front behind which the compact H II region formed.

Subject headings: masers — Zeeman effect

I. INTRODUCTION

Hydroxyl masers associated with H II regions typically exhibit spectra consisting of many features which are predominantly circularly polarized. The Zeeman effect is the simplest explanation for the circular polarization, since mode suppression effects are probably negligible in astrophysical masers.

Identification of Zeeman patterns in OH masers is important because it provides an estimate of the magnetic field in regions of star formation. However, attempts to identify Zeeman patterns have not been straightforward for two reasons. First, no complete Zeeman pattern has been observed. In particular, linearly polarized features associated with the transverse component of the magnetic field are rarely seen. Goldreich, Keeley, and Kwan (1973) show that the growth of linear polarization can be suppressed by the combined effects of resonant radiation trapping and Faraday rotation.

The second problem with the Zeeman interpretation has been that there is no convincing spatial correspondence between left- and right-circularly polarized components in some maser maps, such as the one of W3 (OH) at 1665 MHz (Moran *et al.* 1968; Harvey *et al.* 1974). However, VLBI maps of sources with less complex structure at 1720 MHz (Lo *et al.* 1975) and Orion at 1665 MHz (Hansen *et al.* 1977) show that the strongest features of opposite circular polarization are generally coincident to within a projected distance of 10^{15} cm.

Spectral measurements in circular polarization have been reported for six transitions of OH toward W3 (OH). Zuckerman *et al.* (1972) suggested that certain circularly polarized components in these spectra form parts of Zeeman patterns. They inferred longitudinal magnetic field strengths of about 7 milligauss. Davies (1974) noted that for all six transitions the right-handed features are systematically displaced to higher velocity compared with the left-handed features. The field strength inferred from this general velocity displacement is about 6 milligauss, pointing away from the Earth, the expected direction for the general magnetic field.

In this *Letter* we present the results of a VLBI experiment on the $^2\Pi_{3/2}$, $J = 5/2$, $F = 3 \rightarrow 3$ transition of OH at 6035.093 MHz toward W3 (OH). The spectra we measured are shown in Figure 1. Our map of this source is much more accurate and complete than the one published by Knowles *et al.* (1973) because we used better receivers, maser frequency standards, a longer baseline, circularly polarized feeds, and a correlator having improved spectral resolution. This new map provides the most convincing evidence yet obtained for the Zeeman effect in cosmic masers.

II. OBSERVATIONS AND DATA ANALYSIS

The interferometer elements in this experiment were the 26 m antenna of the Naval Research Laboratory (NRL) at Maryland Point, Maryland, the 43 m antenna of the National Radio Astronomy Observatory

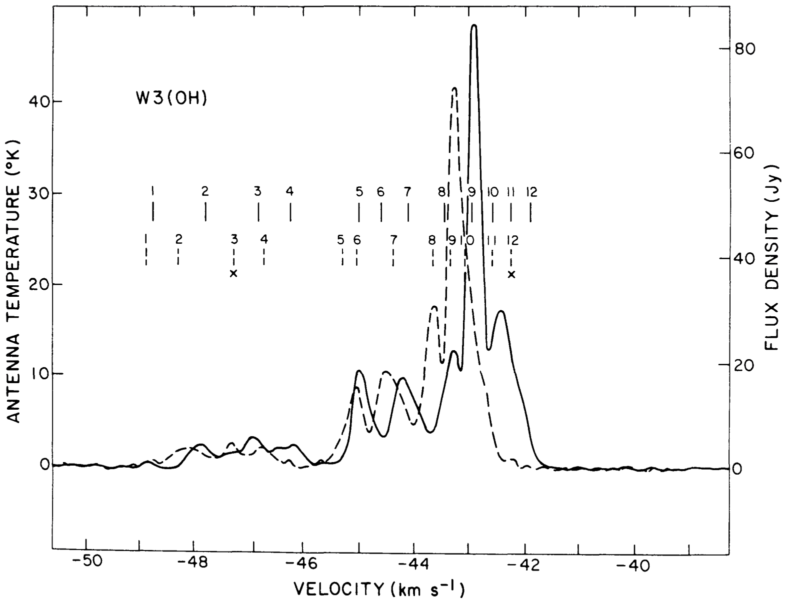

FIG. 1.—Total power spectra of the $^2\Pi_{3/2}$, $J = 5/2$, $F = 3 \rightarrow 3$ transition of OH toward W3 (OH) in (*solid line*) right-circular polarization (RCP) and (*dashed line*) left-circular polarization (LCP). The velocity axis is referred to the local standard of rest and a rest frequency of 6035.093 MHz (ter Meulen *et al.* 1976) which is 8 kHz higher than the one used in most previous work. The spectral resolution with uniform weighting is 2.6 kHz or 0.13 km s^{-1}. The flux density scale in one polarization is calculated as 2.0 Jy K^{-1} for the NRAO antenna. The vertical lines mark the velocities of features identified in the cross-power spectra. The numbers correspond to the entries in Table 1. Features 3 and 12 in LCP were absent in all of the cross-power spectra and could not be mapped.

(NRAO)[1] at Green Bank, West Virginia, and the 46 m antenna of the Algonquin Radio Observatory (ARO) in Algonquin Park, Ontario. All stations had hydrogen maser frequency standards which allowed coherent integrations of 15 minutes. The polarization capabilities were restricted: NRL had linear polarization (LP) only; ARO had left-circular polarization (LCP) and right-circular polarization (RCP); and NRAO had LP, LCP, and RCP. On each of the three days of the experiment, 1977 April 21–23, W3 (OH) was observed for a period of 10 hours. The data were recorded on the standard Mark II system and processed at NRAO. Standard procedures for fringe rate analysis were followed (Moran 1976): the data were averaged to 10 s; the fringe phases were referenced to a feature at -45.0 km s^{-1}; the time series of data were Fourier transformed; a single fringe rate was estimated for each velocity channel; and the fringe rates as a function of hour angle were analyzed to determine the angular offset from the reference feature.

A position was determined for each channel in the spectrum. Maser features were selected for the map which met three criteria: (1) amplitude greater than a threshold value; (2) low rms residual in the fitted position; and (3) constant position over at least two independent channels (since the resolution was 2.6 kHz and the typical line widths were about 10 kHz, four independent estimates could be obtained for an unblended feature). The application of these criteria gives maps that are substantially correct but not necessarily complete. The relative errors (1 σ) among positions of features having the same polarization is typically $0''.025$ in each coordinate but never more than $0''.05$.

The best maps were the ones in circular polarization from the NRAO–ARO baseline. These two maps were aligned on the basis of the positions of three pairs of oppositely polarized features which appeared in the linearly polarized map from the NRAO–NRL baseline. The uncertainty in the alignment of the LCP and RCP maps is $0''.1$ in each coordinate. The results are listed in Table 1 and plotted in Figure 2.

III. ABSOLUTE POSITION

The absolute position of the OH source was determined from data on the NRAO–NRL baseline, because the long-term stability of the ARO frequency standard was poor. The data consisted of 50 measurements of fringe rate: 15 on the maser, and 35 on the calibrator sources 3C 84, 3C 454.3, and 3C 273. The positions of these calibrators were taken as the weighted mean of the positions given by Wade and Johnston (1977) and Clark *et al.* (1976). The effects of a model ionosphere were removed from the data. A least-mean-squares analysis was performed to estimate six parameters: the right ascension and declination of the maser, the two equatorial baseline coordinates, one parameter for the tropospheric model, and a clock parameter. The absolute position of the maser, referred to the -45.0 km s^{-1} RCP feature, is $\alpha = 02^h23^m16^s.42 \pm 0^s.03$, $\delta = 61°38'57''.5 \pm 0''.2$ (1950.0). The errors are 1 σ values which include an allowance for systematic effects.

[1] NRAO is operated by Associated Universities, Inc., under contract with the National Science Foundation.

The OH features project directly onto a very compact H II region studied by Harris and Scott (1976) and Harten (1976). The ground-state OH features also project directly onto the compact H II region, while the water masers are 7″ to the west (Forster, Welch, and Wright 1977). A compact 2 μm IR source (Wynn-Williams, Becklin, and Neugebauer 1972) is probably associated with the H II region, but the positional accuracy is inadequate to confirm this.

IV. DISCUSSION

The map of W3 (OH) shows 12 features in RCP and 10 in LCP. Each of the 10 LCP features can be paired with a nearby RCP feature. There are features in the LCP spectrum (3 and 12) that might be associated with the two unpaired RCP features but they were resolved by the interferometer. The average angular separation among the 10 pairs is 0″.13, which may be partly due to a misalignment in the maps. The mean offset of the RCP from the LCP components can be made equal to zero in each coordinate by moving the LCP components by +0″.11 in right ascension and −0″.05 in declination. This reduces the average displacement between the RCP and LCP pairs to 0″.08. The lack of exact angular coincidence between the RCP and LCP pairs may be mostly due to mapping uncertainties. The close alignment of all of the oppositely polarized features strongly suggests a Zeeman interpretation of the line formation. The longitudinal magnetic fields inferred by the velocity separations range from 2 to 9 milligauss.

For most of the Zeeman pairs listed in Table 1, the flux densities of the two components are approximately equal and the inferred longitudinal magnetic field is close to 9 milligauss. However, for the Zeeman pairs in which one component is more than a factor of 2 stronger than the other, the longitudinal fields appear to be weaker. This behavior can be explained by turbulent magnetic and velocity fields which would make the gain paths different for oppositely polarized components, causing unequal flux densities (see Cook 1966), and would make the average longitudinal magnetic field appear weaker than those measured for less turbulent regions.

Total gas densities in regions of OH masers are generally thought to be about 10^6–10^8 cm^{-3} (Litvak

TABLE 1

Positions and Magnetic Field Strengths for Zeeman Components Identified in W3 (OH)

Zeeman Pair	Velocity* (km s^{-1})	S† (Jy)	V‡	θ_x§ (″)	θ_y§ (″)	$\Delta\theta$‖ (″)	Δv# (km s^{-1})	B** (mG)
1..........	−48.9L	~1	1.0	+1.31	+0.86	0.27	0.1	2
	−48.8R	~1	1.0	+1.50	+0.66			
2..........	−48.3L	3	0.5	+0.15	+0.38	0.05	0.5	9
	−47.8R	4	0.2	+0.19	+0.40			
3..........	−47.3L	5	<0.2	...	...	...	0.5	9
	−46.8R	5	0.6	−0.70	+0.51			
4..........	−46.7L	4	0.6	+0.12	+0.43	0.11	0.5	9
	−46.2R	4	0.8	+0.21	+0.38			
5..........	−45.3L	6	0.5	−0.08	−0.01	0.08	0.3	5
	−45.0R	19	0.7	0.00	0.00			
6..........	−45.0L	14	0.4	+0.08	+0.49	0.14	0.4	7
	−44.6R	6	0.4	+0.20	+0.41			
7..........	−44.6L	16	0.4	−0.40	−1.34	0.30	0.5	9
	−44.1R	17	0.2	−0.15	−1.51			
8..........	−43.6L	30	0.2	0.00	+0.39	0.06	0.2	4
	−43.4R	15	0.3	+0.06	+0.37			
9..........	−43.3L	62	0.3	+0.02	−0.79	0.05	0.3	7
	−43.0R	82	0.3	+0.07	−0.80			
10..........	−43.0L	35	0.6	+0.13	+0.27	0.08	0.4	7
	−42.6R	24	0.4	+0.21	+0.27			
11..........	−42.6L	9	0.4	+0.09	+0.28	0.15	0.3	5
	−42.3R	25	0.4	+0.24	+0.29			
12..........	−42.3L	9	<0.2	...	...	...	0.4	7
	−41.9R	6	0.4	+0.25	+0.30			

Notes to Table 1

* LSR velocity. Letter denotes sense of circular polarization: (L) left; (R) right.

† Approximate flux density.

‡ Peak fringe visibility.

§ The relative errors (1 σ) among positions of features having the same polarization are typically 0″.025 in each coordinate and never more than 0″.05. The relative alignment between the left and right maps is accurate to 0″.1 in each coordinate.

‖ The angular offset between components of each Zeeman pair. The mean offset can be minimized by offsetting the LCP components by 0″.11 in right ascension and −0″.05 in declination.

Velocity separation between components of Zeeman pair.

** Longitudinal magnetic field (B = 16.7 milligauss km^{-1} s). All the fields are directed away from the Earth.

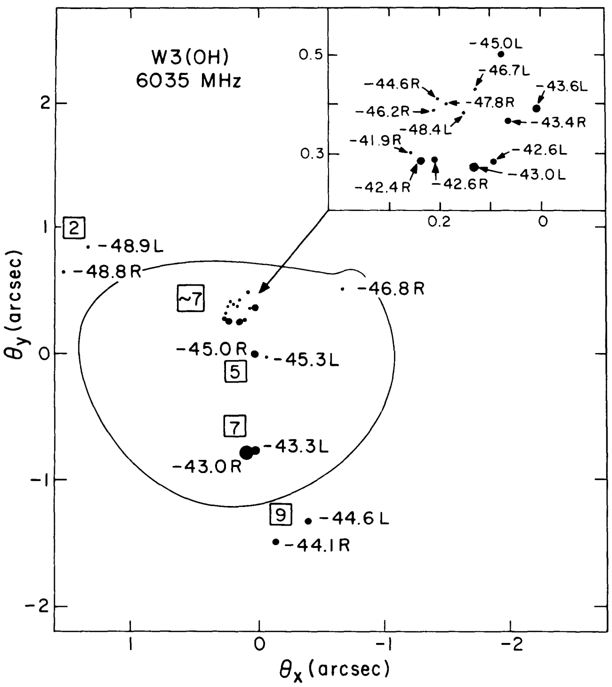

FIG. 2.—Map of the relative positions of the OH maser features toward W3 (OH). The 1 σ error in position among the RCP features is 0."05 or better and the alignment error between the RCP and LCP groups is 0."1. Each spot is labeled by a velocity and sense of circular polarization (L or R) and has a size proportional to the flux density of the corresponding spectral feature. The longitudinal magnetic field strengths in milligauss are shown in the boxes. The contour (2300 K) is from the 15 GHZ map of Harris and Scott (1976), which can be aligned with our map to an accuracy of 0."2.

1973). A density of 10^7 cm^{-3} and field of 6 milligauss for an object condensed from the general interstellar medium (where the density is $\sim$1 cm^{-3} and the field $\sim$1 microgauss) is consistent with a model in which the magnetic field scales proportionally with the square root of the density. This dependence seems reasonable in the light of recent calculations by Mouschovias (1976).

Our observations place constraints on the volume and mass of the masing regions. The projected baseline on the NRAO-ARO interferometer was almost constant in length (1.7×10^7 wavelengths) but varied in orientation. The fringe visibilities were variable, but never larger than 0.4 (for 20 minute averages.) This suggests a typical apparent angular scale size of about 0."005 for the masing components. In an unsaturated maser this would imply a total gain length of about 0."025 or 10^{15} cm at a distance of 3 kpc. Another estimate of the gain length based on the velocity gradients among the features (see Fig. 2) gives the same result. The mass of each maser component is approximately 10^{-5} $M_\odot$ based on a density of 10^7 cm^{-3} and a diameter of 10^{15} cm. Hence each component is probably associated with a small condensation within a single large cloud rather than with a separate protostar.

The close angular correspondence of the maser spots with the position and extent of the compact H II region implies a physical relationship between them. The velocity of the compact H II region is -52 km s^{-1} as determined from recombination lines (Hughes and Viner 1976), and thus the OH masers which lie between -42 and -49 km s^{-1} are clearly redshifted from the velocity of the H II region. Because the H II region is optically thick at 6 GHz (Harris and Scott 1976), the emission we see comes from masers in front of the H II region W3 (OH). Hence the OH maser emission could not be formed in an expanding shell around the compact H II region, since this would require the masers to have velocities lower than -52 km s^{-1}.

The data suggest two dynamical models. The first possibility is that the masers are located within an accretion shell around the exciting star just outside the ionization front associated with the compact H II region. For an infall velocity of 7 km s^{-1} and a diameter of 10^{17} cm the mass of the central object is about 100 $M_\odot$. This mass is reasonable for an O star needed to excite the compact H II region. The compact ammonia cloud with a feature near -44 km s^{-1} may be part of this shell (Wilson, Bieging, and Downes 1978). However, the velocities of the maser features do not fit the pattern expected for a simple collapsing shell. The wide range of velocities represented in the small cluster of features in Figure 2 suggests that the velocity field is dominated by turbulence, possibly caused by the disturbances propagating at the Alfvén speed, which is about 4 km s^{-1} for a magnetic field of 6 milligauss and a density of $\sim 10^7$ cm^{-3}.

In the second model the OH maser clumps are typical components of the extended molecular cloud which are visible as OH masers only because they happen to lie in front of the compact H II region. This is reasonable, since the velocity of the CO emission from the extended molecular cloud around W3 (OH) spans the range of -41 to -51 km s^{-1} with a peak near -48 km s^{-1}. The velocity difference between the H II region and the OH masers is due to the motion of the compact H II region through the molecular cloud. Such relative motion would be expected if O stars formed within shocked layers at the interfaces of molecular clouds and extended H II regions, as proposed by Elmegreen and Lada (1977).

We thank E. Chaisson, B. Elmegreen, and M. M. Litvak for helpful discussions.

REFERENCES

Clark, T. A., *et al.* 1976, *A.J.*, **81**, 599.
Cook, A. H. 1966, *Nature*, **211**, 503.
Davies, R. D. 1974, in *IAU Symposium No. 60, Galactic Radio Astronomy*, ed. F. J. Kerr and S. C. Simonson III (Dordrecht: Reidel), p. 275.
Elmegreen, B. G., and Lada, C. J. 1977, *Ap. J.*, **214**, 725.
Forster, J. R., Welch, W. J., and Wright, M. C. H. 1977, *Ap. J.* (*Letters*), **215**, L121.
Goldreich, P., Keeley, D. A., and Kwan, J. Y. 1973, *Ap. J.*, **182**, 55.

Hansen, S. S., Moran, J. M., Reid, M. J., Johnston, K. J., Spencer, J. H., and Walker, R. C. 1977, *Ap. J. (Letters)*, **218**, L65.
Harris, S., and Scott, P. F. 1976, *M.N.R.A.S.*, **175**, 371.
Harten, R. 1976, *Astr. Ap.*, **46**, 109.
Harvey, P. J., Booth, R. S., Davies, R. D., Whittet, D. C. B., and McLaughlin, W. 1974, *M.N.R.A.S.*, **169**, 545.
Hughes, V. A., and Viner, M. R. 1976, *Ap. J.*, **204**, 55.
Knowles, S. H., Johnston, K. J., Moran, J. M., and Ball, J. A. 1973, *Ap. J. (Letters)*, **180**, L117.
Litvak, M. M. 1973, *Ap. J.*, **182**, 711.
Lo, K. Y., Walker, R. C., Burke, B. F., Moran, J. M., Johnston, K. J., and Ewing, M. S. 1975, *Ap. J.*, **202**, 650.
Moran, J. M. 1976, *Methods of Experimental Physics*, **12c**, ed. M. L. Meeks (New York: Academic), p. 228.
Moran, J. M., Burke, B. F., Barrett, A. H., Rogers, A. E. E., Carter, J. C., Ball, J. A., and Cudaback, D. D. 1968, *Ap. J. (Letters)*, **152**, L97.
Mouschovias, T. Ch. 1976, *Ap. J.*, **207**, 141.
ter Meulen, J. J., Meerts, W. L., van Mierlo, G. W. M., and Dymanus, A. 1976, *Phys. Rev. Letters*, **36**, 1031.
Wade, C. M., and Johnston, K. J. 1977, *A.J.*, **82**, 791.
Wilson, T. L., Bieging, J., and Downes, D. 1978, *Astr. Ap.*, **63**, 1.
Wynn-Williams, C. G., Becklin, E. E., and Neugebauer, B. 1972, *M.N.R.A.S.*, **160**, 1.
Zuckerman, B., Yen, J. L., Gottlieb, C.A., and Palmer, P. 1972, *Ap. J.*, **177**, 59.

K. J. Johnston and J. H. Spencer: Code 7132, E. O. Hulburt Center for Space Research, Naval Research Laboratory, Washington, DC 20375

C. J. Lada and J. M. Moran: Center for Astrophysics, 60 Garden Street, Cambridge, MA 02138

M. J. Reid: National Radio Astronomy Observatory, Edgemont Road, Charlottesville, VA 22901

J. L. Yen: Department of Electrical Engineering, University of Toronto, Toronto, ON Canada